

## **UC Riverside**

### **UC Riverside Electronic Theses and Dissertations**

**Title**

Designed Assembly of Biomimetic Membrane From Amphiphilic Copolymers

**Permalink**

<https://escholarship.org/uc/item/9d38m5xx>

**Author**

Tseng, Chun-Che

**Publication Date**

2011

Peer reviewed|Thesis/dissertation

UNIVERSITY OF CALIFORNIA RIVERSIDE

Designed Assembly of Biomimetic Membrane From Amphiphilic Copolymers

A Thesis submitted in partial satisfaction  
of the requirements for the degree of

Master of Science

In

Chemical and Environmental Engineering

by

Chun-Che Tseng

March 2011

Dissertation Committee:

Dr. Jianzhong Wu, Chairperson

Dr. Wilfred Chen

Dr. Ashok Mulchandani

Copyright by  
Chun-Che Tseng  
2011

The Thesis of Chun-Che Tseng is approved

---

---

---

University of California, Riverside

## Acknowledgment:

Foremost, I would like to express my sincere gratitude to my advisors Dr. Jianzhong Wu and Dr. Wilfred Chen for the continuous support of my study and research, for their patience, motivation, enthusiasm, and immense knowledge. Their guidance helped me in all the time of research and writing of this thesis.

I want to thank Dr. Jianzhong Wu, Dr. Wilfred Chen and Dr. Ashok Mulchandani for being my thesis advisors and their encouragement, insightful comments, and enlightening questions.

Special thanks to Dr. Peter Agre for donating experimental materials, Dr. Yushan Yan and Dr. Sharon Walker for sharing their lab instruments, and Dr. Quan Jason Cheng for his valuable advises.

I also want to thank my fellow labmates: Shen-Long Tsai, Fang Liu, Chaokun Li, Bhawna Madan, Miso Park, Divya Sivaraman, Lakshmi Cella, Garima Goyal, Garima Chaudhary, Qing Sun and Daniel Blackstock for their guidance and stimulating discussions, for the sleepless nights we were working together, and for all the fun we have had in the last two years.

## ABSTRACT OF THE THESIS

Designed Assembly of Biomimetic Membrane From Amphiphilic Copolymers

by

Chun-Che Tseng

Master of Science, Graduate Program in Chemical and Environmental Engineering

University of California, Riverside, March 2011

Dr. Jianzhong Wu, Chairperson

At appropriate condition amphiphilic block copolymers may self-assemble into well-organized mesoscopic structures such as micelles, vesicles, microscopic sheets and rods useful for practical applications. Vesicles of charged amphiphilic block copolymers have been utilized for fabrication of biomimetic membranes that exhibit properties similar to those of biological cell membranes but with exceptional durability and mechanical strength. Such membranes are suitable for embedding proteins/enzymes for various industrial applications.

In this work, amphiphilic block copolymers of complementary charges are used in a cascade self-assembly process that involves sequential formation of vesicles in solution and their fusion on a charged substrate. Each copolymer chain links a strong polyelectrolyte (hydrophilic) block with a hydrophobic polymer that provides the

driving force of the vesicle self-assembly in an aqueous environment. Biomimetic membranes are formed by layer-by-layer deposition/fusion of oppositely charged vesicles at a strongly charged mica surface. The cascade self-assembly process allows us to have a precise control of the membrane microscopic structure, thickness and composition. We have identified optimal solution conditions for formation of various mesoscopic block copolymer structures. The morphologies of cationic and anionic block copolymer structures at dry and at wet conditions are characterized by, respectively, atomic force microscopy (AFM) and by dynamic light scattering (DLS) measurements. Moreover, the thicknesses of these biomimetic membranes on the substrate have been measured by AFM scratching experiments. While the practical utility of these biomimetic membranes is yet to be demonstrated, this work provides deeper understanding of the size variation and spreading of amphiphilic block copolymer vesicles on mica surface and the selection of appropriate conditions for membrane fabrication.

## Table of contents

ABSTRACT OF THE THESIS .....	v
1. Introduction .....	1
1.1 Fusion of block copolymer vesicle .....	4
1.2 Reconstitution of proteins in block copolymer membranes .....	5
1.3 Channel proteins: Aquaporin.....	7
1.4 Polyelectrolyte layer-by-layer assembly .....	8
1.5 Surface charge of the substrates.....	9
2. Experiment and methods.....	11
2.1 Protein expression and purification.....	11
2.2 Block copolymers: PS-PAA and PB-P4VPQ .....	11
2.3 Vesicle self-assembly in bulk phase .....	12
2.4 Substrate preparation .....	13
2.5 Atomic Forced Microscopy (AFM).....	13
2.6 Dynamic Light Scattering .....	14
2.7 Electrokinetic Analyzer.....	14
3. Results and discussions.....	16
3.1 Overexpression of AquaporinZ .....	16
3.2 Morphology of PS-PAA vesicle.....	20
3.3 Spreading of PB-P4VPQ vesicles .....	27
3.3.1 Vesicle deposition on aminoalkylsilane treated glass.....	28
3.3.2 Deposition on silicon oxide.....	30
3.3.3 Deposition on muscovite mica .....	34
Conclusions.....	38
Reference.....	40

## List of figures

Figure 1. Schematic of an amphiphilic block copolymer bilayer membrane embedded with water channel proteins (aquaporin).....	7
Figure 2. The pTrc10HisAqpZ plasmid and double digested product analyzed by agarose gel electrophoresis.....	16
Figure 3. The pTrc10HisAqpZ protein expression resolved by 10% SDS-PAGE..	17
Figure 4. Dissociation of the SDS-resistant pTrc10HisAqpZ..	18
Figure 5. The morphology of block copolymer (PS-PAA) vesicles in different concentration and water content..	24
Figure 6. The graph of the size variance of the block copolymer PS-PAA vesicles in different conditions. ....	26
Figure 7. AFM image of the silane coated glass after deposition of the vesicular dispersions. ....	29
Figure 8. AFM image of the silicon oxide surface deposited the PB-P4VPQ solution. ....	32
Figure 9. AFM image of the surface deposited the block copolymer vesicular dispersions. ....	34
Figure 10. AFM image of the muscovite mica surface after deposited the 0.1 % PB-P4VPQ vesicular dispersion..	36
Figure 11. The surface histogram analysis of the mica surface deposited with copolymer vesicular dispersion. ....	37

## List of tables

Table 1. The average size of block copolymer PS-PAA vesicles measured by Dynamic Light Scattering. .....	25
Table 2. Contact angle measurement of different substrates.. ..	28

## 1. Introduction

A block copolymer consists of at least two distinct polymer identities linked by covalent bonds[1]. Diblock copolymers are those with two blocks, triblock copolymers with three blocks, and so on for multiblock copolymers. The size, chemical composition and characteristics of block copolymers can be easily customized by selection of desired monomers and the degree of polymerization.

Like small molecule amphiphilic surfactant systems, block copolymers can form a wide variety of mesoscopic structures with well-defined morphologies[2] in the bulk phase or in dry state. In particular, amphiphilic block copolymers attract lots of attentions in both academia and industry because of their compatibility with an aqueous environment and a wide range of parameters for control of the size [3], chemical composition[4], and morphologies of self-assembled structures in the bulk phase or under confinement. When dissolved in water, amphiphilic block copolymers tend to self-assemble into well-defined structures with the insoluble polymer cores covered by the soluble polymer parts[5]. The microscopic structure depends on the solution condition including pH and salt concentration, the polymer molecular weight, the chemical composition and relative solubilities of the individual monomers. As block copolymer melts, amphiphilic block copolymers can form

numerous nano-scale structures such as micelles, vesicles, microscopic sheets or rods.

Amphiphilic block copolymers provide a wide range of parameter space for fabrication of novel nano-scale structures. In general, their self-assembly is more tolerant to different chemicals mixed in the system than conventional amphiphilic surfactants or lipids. The better durability and chemical resistance make amphiphilic block copolymers a good candidate for novel applications[6] such as nano-sized carriers for drug delivery[7], selective permeable membranes[8], and growth of carbon nanotubes[9].

Like surfactants, amphiphilic block copolymers may self-assemble into vesicles, a closed bilayer structure. Also analogous to small molecular systems, vesicles of phospholipids are referred to as liposomes, vesicles of block copolymers are often designated as polymersomes. Whereas small- molecule vesicles are often spherical, polymersomes can form vesicles of other shapes and can be unilamellar or multilamellar. For example, vesicles of amphiphilic diblock copolymer normally have ABA or ABBA structures where A represents water loving block and B represents oily block. When dissolved in water or aqueous solutions, the oily parts of the amphiphile copolymer tend to aggregate together to limit the contact area with the solvent

while the hydrophilic parts face inner and outer solution[4]. Compare to micelles, vesicles may not be thermodynamically stable. Another important difference between vesicles and micelles is that the vesicles have an inner space that encloses some of the aqueous solution. At very low polymer concentration, an amphiphilic diblock copolymer always starts from forming micelles then transition into vesicles when increasing the concentration.

Previous studies have shown that block copolymer membranes are usually at least 2-folds thicker than lipid membranes and perform better mechanical stability and chemical resistance. These advantages make block copolymers an ideal candidate for biomimetic membranes that can be used for membrane protein reconstitution. It has been shown that the membrane proteins remain fully functional even embedded in the artificial polymer environment[10]. The protein-polymer membranes have incredible potential for water treatment, purification[11], nanoreactor[12] and drug delivery[13].

## **1.1 Fusion of block copolymer vesicle**

Many techniques have been developed for membrane fabrication from surfactants or lipids. These include Langmuir-Blodgett(LB) technique[14], spin coating[15], and self-assembled monolayer (SAM)[16]. While they are powerful for making membranes of small molecules, conventional techniques met some obstacles for fabrication of block copolymer membranes. For example, the Langmuir-Blodgett method is a clever way to fabricate single-layer or multiple-layer membranes, but this technique requires high-cost instrument and only the amphiphilic materials are applicable. Moreover, the product is unsustainable in dry state[17]. While the spin coating method is an easy and low cost method which is commonly used to engineer planer polymer layers, there is no literature on formation of the desired bilayer structure by this technique. The SAM method can be utilized in many materials on several substrates such as gold, silicon oxide (glass), metals or mica, but this technique can only be applied to engineering monolayer structure.

Vesicle fusion method has been widely used in planar lipid bilayer membrane fabrication[18]. Vesicle spreading on a solid substrate requires accurate tuning of the solution condition in order to obtain the desired homogeneous planar lipid bilayer without structural disorder and flaws[19]. The vesicle fusion method is in particular

attractive for fabrication of amphiphilic block copolymer membranes. First, low molecular weight amphiphilic diblock copolymers tend to have similar properties as lipids. Second, the amphiphilic block copolymers can be designed to target the desired structure by tuning the block composition and molecular weight[20]. Third, amphiphilic block copolymers tend to have strengthened durability and mechanical stability, and better chemical resistance. These properties make amphiphilic block copolymer an ideal candidate for fabrication of novel permeable membranes. A major goal of this work is to develop an experimental protocol for synthesis of planar amphiphilic block copolymer membranes by the vesicle fusion method.

## **1.2 Reconstitution of proteins in block copolymer membranes**

Membrane proteins isolated from cells can be reconstituted into off-cell systems such as vesicles[11] or black lipid bilayers[21]. Depending on their innate biological functions, membrane proteins would perform channels for transporting small molecules, metal ions, protons, either selectively or non-selectively[20]. The transporting route can be controlled by the difference in osmotic pressure or an external electric potential. Otherwise, the transport will be bidirectional[22]. Where there is a good literature demonstrating successful reconstitution of membrane

proteins in stabilized lipid membranes, the durability of planar lipid membranes would decrease with time, thus not suitable for industrial usage[20].

Another drawback of recombinant proteins in lipid membrane is incompatibility of thickness. The thickness of a typical lipid bilayer membrane is around 4 nm, which is similar to the length of membrane protein. Theoretical analysis has shown that proteins incorporated into lipid vesicles would easily cause the unsteadiness of the system, which leads to the structural disorder or deformation [23]. The structure instability was caused by the physical properties of lipid bilayer membranes. In comparison to lipid bilayer membranes, amphiphilic block copolymer membranes are rather incompressible. As a result, even a small thickness change caused by the insertion of membrane proteins would cause a huge energy penalty which disturbs the incorporation of proteins into the membrane.

As amphiphilic block copolymer materials attract more and more attentions, many researchers have recognized the advantages of polymersomes than liposomes as the transporters for drug delivery. As aforementioned polymersomes have strengthened mechanical steadiness and better flexibility to form polymer bilayer structures[24]. However, the thickness of typical block copolymer bilayer is located between 8-12 nm, which means two to three times thicker than the average

thickness of conventional lipid bilayers, therefore, the greater thickness was thought too large for a off-cell system in order to embed membrane proteins. Nevertheless, a theoretical study by Pata et al.[25] Indicates that it is feasible to incorporate membrane proteins into block copolymer membranes. Moreover, Meier et al. have successfully embedded membrane protein AqpZ in amphiphilic block copolymer vesicles [11]. These authors have also shown that the AqpZ remained its water permeability in vesicle phase[11]. Both theoretical and experimental results suggest that the recombination of membrane protein into planar block copolymer membrane is achievable.

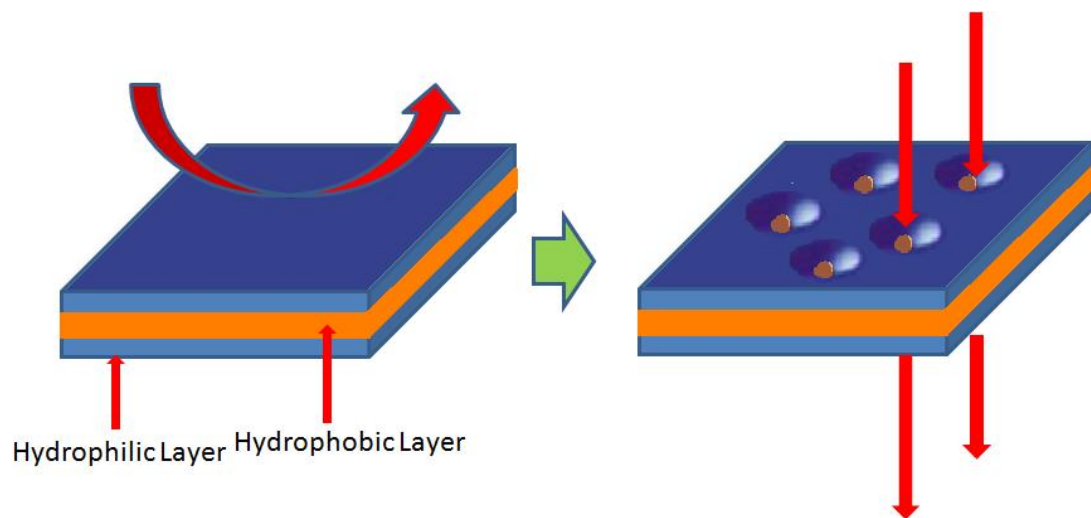


*Figure 1. Schematic of an amphiphilic block copolymer bilayer membrane embedded with water channel proteins (aquaporin). Left figure represents the water impermeable membrane. Right figure represents after embedded with water channel proteins, water molecules can flow through the aquaporin water channels.*

### **1.3 Channel proteins: Aquaporin**

Membrane transporting proteins play critically physiological roles in living cells: they are regarded as the bridge between the cytoplasm and the extracellular environments[26]. Aquaporins are common water channel proteins embedded in the cell membrane that control the transportation of water and small molecules. They are characterized by extraordinary water permeability and low activation energy[27]. Literature has shown that, after reconstituting into proteoliposomes, AquaporinZ exhibits impressive water permeability ( $P_f=10 \times 10^{-14} \text{ cm}^3 \text{ s}^{-1}$  per subunit) and has low Arrhenius activation energy ( $E_a=3.7 \text{ kcal/mol}$ ). Under ideal conditions 12 ng of AquaporinZ is able to recover 2.4 liter of water, enough for daily consumption of a single person [28]. Aquaporins exist in mammals, plants[29], prokaryotes[30] etc. In plants, they also play an important role of the protecting mechanism against freeze-thaw stress[31]. In this study, we choose AquaporinZ (AqpZ), a water channel protein which found in *Escherichia coli strains*. It has been shown that AqpZ can be embedded into off-cell systems such as lipid vesicles and block-copolymer membranes[11] and maintains its function of extraordinary water permeability.

#### **1.4 Polyelectrolyte layer-by-layer assembly**

The technique of fabricating layer-by-layer polymer membrane provides a fast, low cost and a straightforward way to fabricate polymer multiple layers. The preparation and procedure of layer-by-layer deposition is quite simple. In an aqueous environment, many substrates are slightly charged. For example, glasses, mica and quartz are negatively charged in water. When a negatively charged substrate is dipped into a solution containing cationic polyelectrolyte, such as poly(acrylamide) (PAA) or poly(diallyldimethylammonium chloride) (PDMA), and removed the excess materials by washing, the net charge of the substrate turns into positive due to the adsorption and overcompensation of cationic polyelectrolytes[32]. If the coated substrate is then dipped into a solution containing negatively charged polymer such as poly(acrylic acid) (PAA), poly(sodium acrylate) (PSA), the anionic polyelectrolyte would be deposited on the outer layer, and the total net charge of the substrate will become negative. By repeating this protocol, one would obtain multiple layers of the alternatively charged polymers on a single substrate, thus achieving thickness control and surface charge control.

### **1.5 Surface charge of the substrates**

In order to understand the effect of the substrate charge on spreading of the block copolymer vesicles, electrokinetic analyzing experiment was performed to measure the zeta potential of the substrates. Because solid materials of any size and shape with instinctively charged would form an electrochemical double layer in a liquid solution, the contact interface between the surface of the material and the liquid solution is covered by a "charged skin"[33]. The formation of this "charged skin" is called the electric double layer (EDL). Intuitively, an EDL consists of two parts: the immobile stern layer near the solid surface and followed by a diffuse layer of mobile ions. When there is a relative motion of the substrate against the liquid solution, these two different layers are separated by a shear plane. Motions or microfluid movements may cause alteration of the charged skin. During the relative motion of the mobile layer towards the fixed charged surface (immobile, solid surface), the zeta potential can be measured[34].

## **2. Experiment and methods**

### **2.1 Protein expression and purification**

The plasmid allowing overexpression of histidine-tagged AquaporinZ (pTrc10HisAqpZ) was kindly donated by Dr. Peter Agre (Molecular Microbiology and Immunology, John Hopkins)[27]. The expression vector was transformed into the commercially available *E. Coli* strain JM109, and grown in lysogeny broth (LB) medium which the colony was selected by ampicillin resistance. The production of proteins was induced by addition of isopropylthiogalactodise (IPTG), different IPTG concentrations and induction time was used in this study in order to find out the optimized condition.

Protein purification was performed by using nickel affinity chromatography, the product of purification was analyzed by 10 % SDS-PAGE. For positive control, *E. Coli* strain BL21 with Dockerin AT was growing in LB medium which the colony was selected by Karamycin resistance, the production of Dockerin was induced by 1 mM IPTG for 2 hours in 37 ° C.

### **2.2 Block copolymers: PS-PAA and PB-P4VPQ**

In this study, two amphiphilic diblock copolymers were used, poly (styrene)-block-poly (acrylic acid) (PS-PAA) ( $M_{n, PS} = 26000 \text{ g mol}^{-1}$ ,  $M_{n, PAA} = 1000 \text{ g mol}^{-1}$ ;  $M_w/M_n = 1.18$ ) and poly (butadiene(1,4 addition)-block-poly (methyl 4-vinyl pyridinium iodide) (PB-P4VPQ) ( $M_{n, PB} = 120000 \text{ g mol}^{-1}$ ,  $M_{n, PAA} = 28200 \text{ g mol}^{-1}$ ;  $M_w/M_n = 1.08$ ), both purchased from Polymer Science Inc. Both block copolymers were used directly without any modification.

### **2.3 Vesicle self-assembly in bulk phase**

In order to prepare uniform sized amphiphilic block copolymer vesicles, 100 mg of PS-PAA was first dissolved in 1 mL of dimethylformamide (DMF, Fisher Scientific Inc.) to form 10 % stock solution, the PB-P4VPQ was dissolved in tetrahydrofuran (THF, Sigma-Aldrich Inc.) to prepare 10% of stock solution. Then the stock solutions were diluted with same solvent to the desired concentrations. Deionized water at the constant rate of one drop every 10 seconds was added to the solution with continues stirring. Deionized water was added to the solution until the desired water/organic solvent ratio was achieved. In order to obtain the uniform sized vesicles, the resulting dispersions were extruded through 0.45  $\mu\text{m}$  syringe filters (Fisher Scientific Inc.).

## **2.4 Substrate preparation**

In this study, three substrates were used for the vesicle deposition, silicon oxide substrates and aminoalkylsilane coated glass substrates were purchased from Fisher Scientific Inc. These substrates were washed by ultrapure water (18.2 M $\Omega$ , Millipore) and dried in the desiccators before used. Muscovite mica (V-1 grade, Ted Pella Inc.) was cleaved and washed by ultrapure water (18.2 M $\Omega$ , Millipore) and then dried in the desiccators before used. The contact angle measurement was performed on these samples (see Table 2).

## **2.5 Atomic Forced Microscopy (AFM)**

AFM measurement was operated on an Innova Scanning Probe Microscope system (Bruker Corporation). All measurements were operated in tapping mode in dry state. For scanning and imaging studies, non-conductive silicon nitride probes (NP-S10; Veeco Ins.) with a spring constant 0.32 N/m were utilized. The cantilever was operated at frequencies between 9 and 14 kHz and typical scan rates ranged from 0.8 to 1.2 Hz.

For the measurements, samples were prepared by placing the filtered vesicle solution on air-dried substrate and carefully washed with ultrapure water. Samples were placed in the desiccators for different time depends on the requirement, all the measurements were performed on dry samples.

## **2.6 Dynamic Light Scattering**

The dynamic light scattering experiments was performed by using a commercial goniometer equipped with a He-Ne laser (wave length 633nm) at scattering angles between 30 ° and 150 ° .

## **2.7 Electrokinetic Analyzer**

The zeta potential experiment was performed by using the Electrokinetic Analyzer (EKA; Anton Paar). All samples were analyzed after rinsed by 2 liters of ultrapure water.

The zeta potential measurement of the charged surface is based on a streaming potential/streaming current ( $dU/dp$ ;  $dI/dp$ ) method. An electrolyte solution was pumped via an electrolyte circuit through the measuring cell which contained the sample. Due to the pressure difference and the relative movement of the charges in

the electrochemical double layer, the streaming potential can be detected via electrodes placed at both sides of the sample.

### 3. Results and discussions

#### 3.1 Overexpression of AquaporinZ

The plasmid allowing overexpression of histidine-tagged AqpZ (pTrc10HisAqpZ) was transformed into the *E.Coli* strain JM109. The product was first examined by gel electrophoresis after double digestion by enzymes EcoR1 and Sal1. Figure 2 shows that, after double digestion, the digested plasmid pTrc10HisAqpZ results in two bands on agarose gel, size 1800 and 10000 base pairs. The size of these two bands matched those reported in the literature[27], suggesting that the plasmid was the desired one.

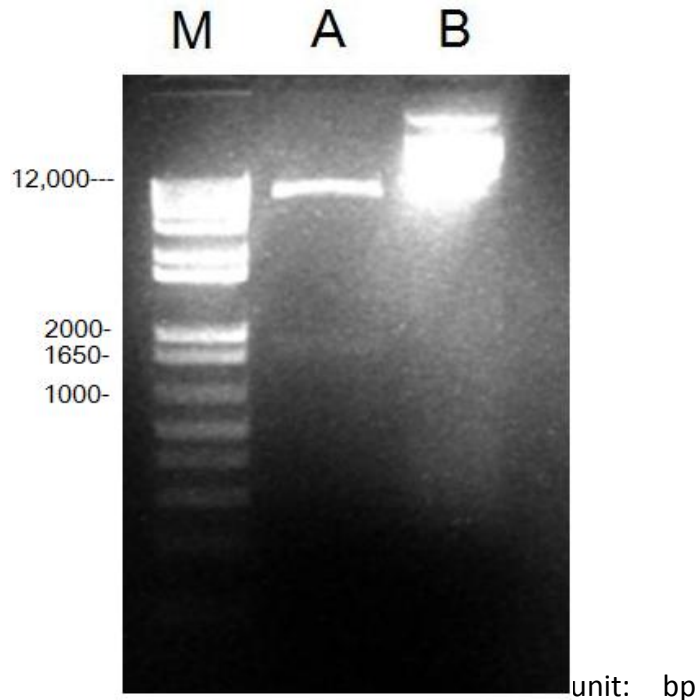


Figure 2. The pTrc10HisAqpZ plasmid and double digested product analyzed by agarose gel electrophoresis. (M) 1 Kb Plus DNA Ladder; (A) pTrc10HisAqpZ digested with enzymes EcoR1 and Sal1; (B) pTrc10HisAqpZ with no digestion

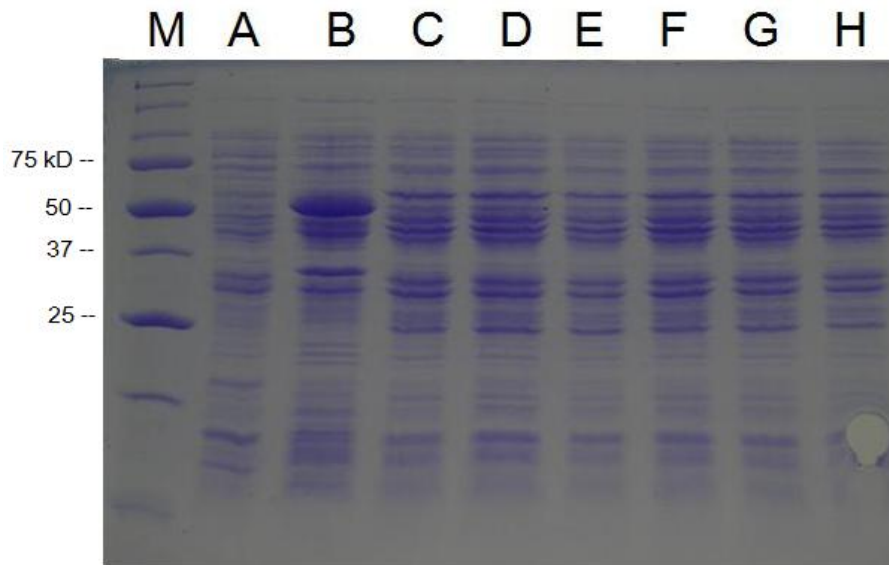
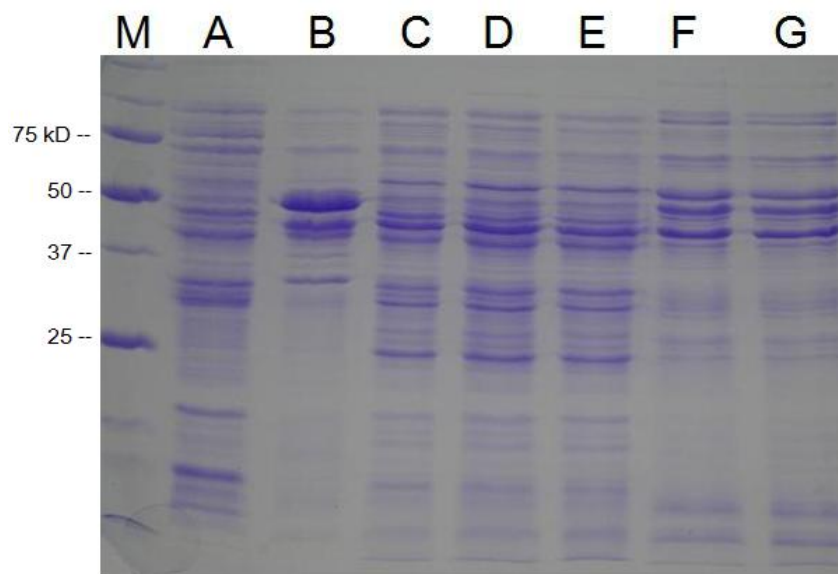


Figure 3. The pTrc10HisAqpZ protein expression resolved by 10% SDS-PAGE. (M) marker; (A) negative control, *E. Coli* strain JM109 without plasmid. (B) positive control for western blotting, *E. Coli* strain BL21 with Dockerin AT. (C) to (H) analysis of pTrc10HisAqpZ in different conditions. (C) cell incubated in 30 °C. (D) incubated in 30 °C, induction for 8 hours. (E) incubated in 25 °C. (F) incubated in 25 °C, induction for 8 hours. (G) incubated in 20 °C. (H) incubated in 20 °C, induction for 8 hours.

Usually the expression level of membrane proteins would be too low to be collected for further applications. It has been reported that the excess amount of membrane protein embedded in cell membranes would affect the structure of cells. The overexpression would lead to dramatic decreasing in cell growth, or immediate cell disruption[35]. Therefore, in order to obtain a sufficient amount of AquaporinZ for purification and further experiments, cell cultures were propagated to higher cell density ( $A_{600\text{ nm}}$  of 2) prior to induction.

Different inducing temperatures (20 °C, 25 °C and 30 °C) were performed to find out the optimal condition for protein overexpression. The induction time was

controlled to 8 hours. The aquaporins migrated as 25-30 kDa monomers during SDS-PAGE. Figure 3 shows that, no significant band appears after induction for all the three inducing temperatures. No band was detected in the Western Blotting test (figure not shown) as well. And this result implied either the expressed amount of AquaporinZ was too low and thus not detectable or the AquaporinZ was not expressed in all the experiments. Different concentrations of inducing agent (IPTG, 0.1 to 1 mM) were used to express the AquaporinZ but no band was detectable in both SDS-PAGE and Western Blotting.



*Figure 4. Dissociation of the SDS-resistant pTrc10HisAqpZ. (M) marker; (A) negative control E. Coli JM109; (B) positive control for western blotting, E. Coli strain BL21 with Dockerin AT; (C) pTrc10HisAqpZ, no induction; (D) induced pTrc10HisAqpZ; (E) induced pTrc10HisAqpZ, Incubated in 500 mM  $\beta$ -mercaptoethanol for 1 hr; (F) membrane fraction recovery; (G) membrane fraction recovery, Incubated in 500 mM  $\beta$ -mercaptoethanol for 1 hr.*

Literatures have already proven that the membrane proteins will aggregate and the aquaporins tend to form tetramers in some conditions, such as normal human body temperature or higher temperatures in the presence of chaotropic (8 M urea or guanidinium chloride) or hydrophilic reducing agents (140 mM  $\beta$ -mercaptoethanol or 100 mM dithiothreitol) or in pH higher than 5.6. The size of the tetramer is around 80 kDa during SDS-PAGE. It was possible that the size of the macromolecular assembly of AquaporinZ was too big to cause the aggregation of AquaporinZ which failed to enter the separating SDS-PAGE gels. Therefore, after the cell induction, higher concentration of hydrophilic reducing agents (500 mM  $\beta$ -mercaptoethanol) was added into the cell culture and incubated for one hour[27] to examine the existence of the AquaporinZ tetramer.

Figure 4 shows that no significant band was detected after incubation in hydrophilic reducing agents for one hour in room temperature. Membrane fraction recovery[27] did not detect any significant band after induction as well. No signal was detected in the Western Blotting test (figure not shown), implying that the AquaporinZ was not overexpressed in all the tests.

The overexpression of membrane protein is usually difficult due to the higher portion of membrane protein which would cause the disruption of the cells and the

insertion machinery may be blocked which would affect the establishment of correct topology of membrane proteins[36].

### **3.2 Morphology of PS-PAA vesicle**

The morphology of the block copolymer (PS-PAA) vesicles in different conditions was examined by Atomic Force Microscopy (AFM). All of the samples were analyzed after desiccating in the vacuum. No aggregate was found when the concentration of block copolymer PS-PAA below 0.0001 %, and the Dynamic Light Scattering analysis did not detect any particles in the samples (detect limit: 5 nm), which indicates that the critical micelle concentration (CMC)[37] of PS-PAA was located between 0.001%-0.0001%.

The block copolymer tends to self-assemble and the solution becomes turbid when the water content is greater than 5%. The vesicle phase starts to appear when the water content reaches 15%. The solute was first dissolved in DMF, water was added drop by drop until the desired ratio. AFM analysis was taken in different water contents, 15% 25%, 35%, and different block copolymer concentrations, 1%, 0.1 %, 0.01 %, 0.001 % and 0.0001%. This analysis gave us more information to understand

the size and phase variance of the amphiphilic block copolymers when changing the solution composition.

When the concentration of the amphiphiles reaches CMC (critical micelle concentration), the PS-PAA molecules tend to aggregate to form micelles, then they will transform into the vesicle phase by increasing the block copolymer concentration. The average diameter of the micelles usually varies from 5 nm to 20 nm due to the limited inner space and single layer spherical structure. The diameters of the vesicles vary from 20 nm to micrometer scale[38]. Figure 5 shows that when the water content remains at 15%, aggregates were found when the polymer concentration reaches 0.001%. Both the AFM and DLS analysis verify the existence of a vesicle phase. The diameter of vesicle measured by DLS was 350.3 nm; which is in good agreement with the diameter measured by AFM image (309.0 nm). The average size of vesicles dropped down to 91.7 nm (measured by DLS) when the block copolymer concentration was 1%. The AFM analysis and DLS measurements were also taken at higher water contents: 25 % and 35 %. The AFM images indicate that, when the water content was maintained at 25 %, the vesicle phase appears at concentration of PS - PAA 0.001 %. The vesicle size varied between 84.5 nm and 111.8 nm when the concentration of PS-PAA is reduced below 0.1 %. The average

size of vesicles increases to 245.3 with increasing the concentration of PS – PAA to 1 %.

Similar phenomenon was found in the system containing 35 % of water. The average diameter of vesicle was found to be 122.8 nm at 0.001 % PS-PAA, and the average diameter measured by AFM increases to 179.9 nm when the BCP concentration reaches 0.1 %.

At some conditions (e.g. 0.01 % of PS-PAA at 35 % of water), the vesicle diameters measured by AFM and DLS are different e almost by 2-folds. This difference might be due to a wide range of size distribution of vesicles in the solution. In other words, vesicles in the solution exist in different diameters. Only the smaller vesicles were found in the AFM analysis.

A similar result was found at higher polymer concentrations: 0.01 % and 0.1 %, indicating that the vesicles are not uniform. When the concentration of PS - PAA reached 1%, the average size of the vesicles was 88.4 nm from AFM analysis, and 91.7 nm from DLS. The polydispersity was 0.16, indicating that the PS-PAA vesicles are more uniform.

According to a theoretical simulation[39], the size change of the vesicles should be directly proportional to the block copolymer concentration change[40]. In other

words, by increasing the block copolymer concentration, the size of the vesicle should also increase[41]. Regrettably, the theoretical prediction was not supported by our experimental results. Figure 5 shows that the average size measured by DLS and by AFM did not change with the PS-PAA concentration. This result was also contradictory to those reported in the literature[41]. The different trend might be caused by aggregation of amphiphiles. When the system is diluted with pure water, the solution first becomes turbid, suggesting self-aggregation of the amphiphilic block copolymers. We suspect that the micelle or vesicle subunits keep aggregating into larger aggregates. Aggregation and precipitation happen throughout the process, leading to the wide range of size distribution.

Table 1 and Figure 6 summarize the experimental data measured by DLS. The results correspond to solution conditions with 55 %, 75 %, 85 % and 95% of water in 0.0001 % of BCP systems. At these conditions, the highest CMC (critical micelle concentration) is about 0.0001 %. As the water content changes from 55 % to 95 %, the diameter of the vesicles varies irregularly during the increasing of the BCP concentration from 0.001 % to 0.1 %. Nevertheless, the vesicle diameter clearly increases when the BCP concentration reaches 1 %. Accordingly, we conjecture that the size of PS-PAA vesicle may be varied section by section. The PS-PAA vesicles are

distributed in a smaller size range when the BCP concentration is below 1 % .The diameter of vesicles is between 150 nm to 250 nm in 45 % of water system. When the concentration of BCP reaches 1 %, the size of the vesicles ascends to higher stage. The diameter of vesicles in 45 % of water went up to 332.8 nm when the BCP concentration attains 1 %.

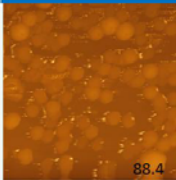
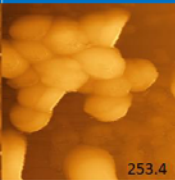
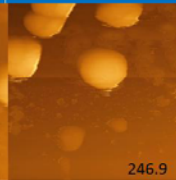
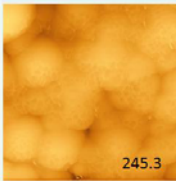
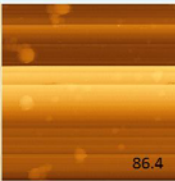
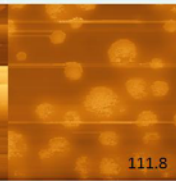
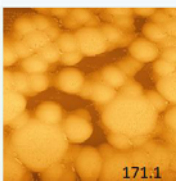
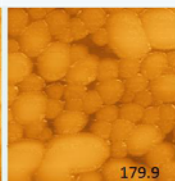
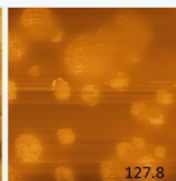
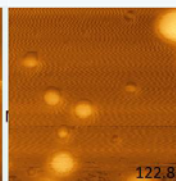
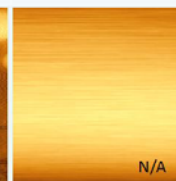
	1% BCP	0.1% BCP	0.01% BCP	0.001% BCP	0.0001% BCP
AFM image of 15% water					
DLS	91.7 nm	295.8 nm	311.0 nm	350.3 nm	N/A
AFM image of 25% water					
DLS	218.5 nm	106.3 nm	123.7 nm	104.7 nm	N/A
AFM image of 35% water					
DLS	189.8 nm	229.6 nm	210.4 nm	146.2 nm	N/A

Figure 5. The morphology of block copolymer (PS-PAA) vesicles in different concentration and water content, DMF was used as cosolvent. The numbers at the bottom-right of each figure indicated the average size of the vesicles in each figure. The dimension of each figure was  $1 \mu\text{m}^2$ . DLS indicates the particle size measured by Dynamic Light Scattering analyzer.

BCP conc. \ water %	15%	25%	35%	45%	55%	
1 %	91.7	218.5	189.8	332.8	262.6	
10 <sup>-1</sup> %	295.8	106.3	229.6	172.2	153.5	
10 <sup>-2</sup> %	311.0	123.7	210.4	188.6	146.5	
10 <sup>-3</sup> %	350.3	104.7	146.2	143.0	138.8	
10 <sup>-4</sup> %	N/A	N/A	N/A	N/A	0.8	
BCP conc. \ water %	65%	75%	85%	95%		
1 %	210.6	206.9	213.8	120.9		
10 <sup>-1</sup> %	142.0	106.0	90.3	89.6		
10 <sup>-2</sup> %	106.5	84.0	65.6	60.2		
10 <sup>-3</sup> %	118.6	114.0	80.8	65.5		
10 <sup>-4</sup> %	N/A	130.3	122.6	52.7		Unit: nm

*Table 1. The average size of block copolymer PS-PAA vesicles measured by Dynamic Light Scattering. Left column indicates the weight percentage of PS-PAA; top column indicates the water ratio in the system.*

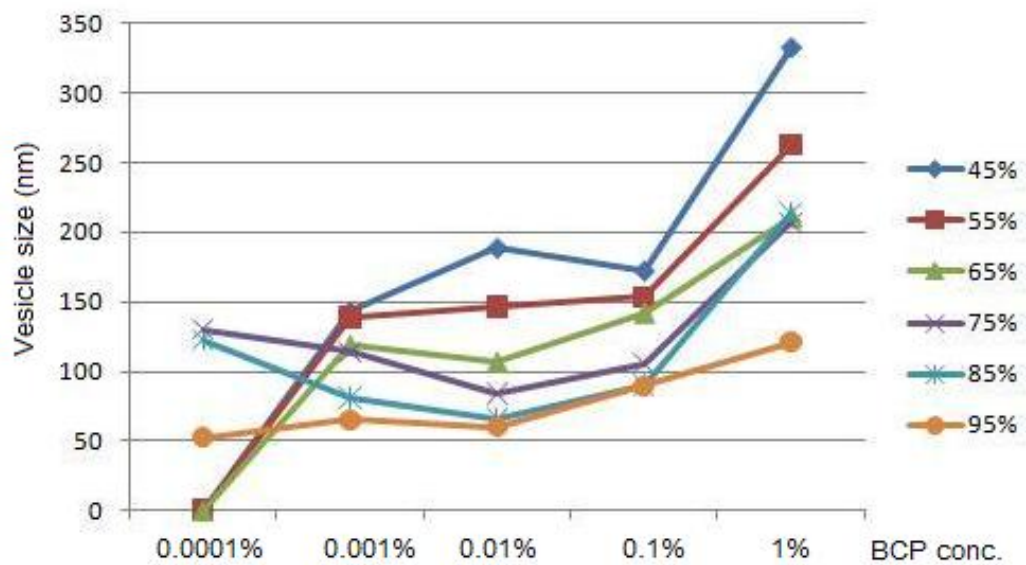


Figure 6. The graph of the size variance of the block copolymer PS-PAA vesicles in different conditions. X-axis indicated the percentage of water; Y-axis indicated the average diameter of PS-PAA vesicles.

### 3.3 Spreading of PB-P4VPQ vesicles

Amphiphilic block copolymer PB-P4VPQ consists of a polybutadiene (PB) block and a poly (methyl 4-vinyl pyridinium iodide) (P4VPQ) block. The PB block is rather hydrophobic and the P4VPQ block is a cationic polymer ( $pK_a = 7.4$ ) that is rather hydrophilic. In other words, the surface of the PB-P4VPQ vesicles (solvent contacted layer) bears positive charges when they are suspending in an aqueous solution. The block copolymer was chosen because the charge on P4VPQ block would help the PB-P4VPQ vesicles to spread on negatively charged substrates due to electrostatic interactions. The strength of the electrostatic forces was mostly determined by the surface charge density of the substrates.

Three different charged substrates were performed in order to observe the spreading efficiency on different surfaces: silicon oxide, muscovite mica, and aminoalkylsilane prepared glass. These surfaces are slightly different in terms of hydrophilicity, surface charge density and polarity. While silicon oxide substrate is slightly anionic charged[42], the surface charge density is sensitive to the pH variance. Muscovite mica ( $KAl_2(Si_3AlO_{10})(F, OH)_2$ ) has high strength of negative surface charge and is most hydrophilic. Aminoalkylsilane coated glass is a hydrophobic and positive charged surface at solution pH 6.3 ( $pK_a = 10.8$ ). All the parameters were maintained during the AFM measurements, such as pH of the solution (pH = 6.3) and temperature ( $20 \pm 2^\circ\text{C}$ ).

Substrate	Contact angle, degree
Aminoalkylsilane prepared glass	71.6 ° ± 1.4 °
Silicon oxide (glass)	44.5 ° ± 2.6 °
Muscovite mica, V-1 grade	< 1 °

*Table 2. Contact angles of different substrates. 0.5  $\mu$ L ultrapure water was used for each analysis.*

### *3.3.1 Vesicle deposition on aminoalkylsilane treated glass*

Vesicle spreading method is commonly used for lipid bilayer fabrication but it has not been used for block copolymer vesicles. The desired amount of PB-P4VPQ was dissolved in THF, water was added drop by drop until the desired ratio. The PB-P4VPQ solution was added on silane treated glass in order to examine the morphology of vesicle dispersion on different surfaces. The silane treated glass carries positive charge in pH=6.3. The contact angle of aminoalkylsilane prepared glass is 71.6 °, indicating that this substrate was rather hydrophobic. The repulsion caused by the same charge would limit adsorption of the cationic polyelectrolyte PB-P4VPQ vesicles on the hydrophobic substrate.

According to the AFM image shown in Figure 7, the vesicles collapse on the silane treated substrate due to the solvent evaporation from the inner space of the vesicle. Solvent evaporation leads to a “donut” structure. The average diameter of the donut structure was between 45 - 55 nm, indicating that the vesicles in the bulk phase have a uniform size. The donut structure also indicates that deposition of 0.1 wt % of PB-P4VPQ solution would not cause the vesicle adsorption and fusion on the

hydrophobic surface. The vesicles did not spread due to several reasons. First, the hydrophobic surface was not favored by the hydrophilic P4VPQ layer that allows the surface immobilization. Second, the positive charge of the silane treated glass render repulsive interactions to the cationic vesicles, which make the PB-P4VPQ vesicles remaining the spherical structure when attaching to the surface. The spherical vesicles are transformed to the donut structure because of the evaporation of the inner solvent.

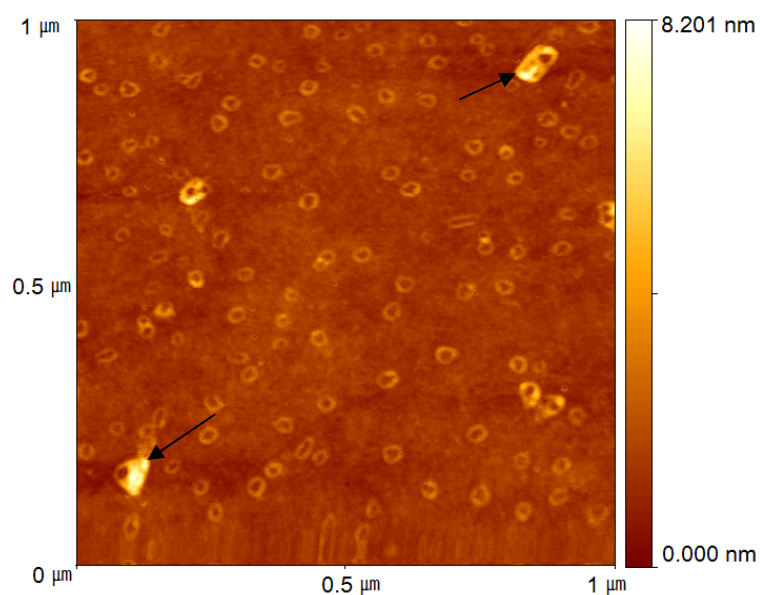


*Figure 7. AFM image of the silane coated glass after deposition of the vesicular dispersions. Image: deposition of the 0.1 % PB-P4VPQ in THF solution contains 50 % water on the silane coated glass. Image revealed numerous collapsed copolymer vesicles (donut-like structure).*

### 3.3.2 Deposition on silicon oxide

The silicon oxide substrate is hydrophilic (contact angle: 44.5 °, Table 2) and carries a charge density of  $-0.15 \times 10^{18} \text{ e}^-/\text{m}^2$ [43] at pH= 6.3. The silicon oxide surface was used for in this work because P4VPQ is a strong cationic polymer in that pH ( $pK_a = 10.8$ ). We expect the electrostatic interaction would lead to vesicle adsorption and spreading on the silicon oxide surface.

According to theoretical calculation, the length of a fully stretched PB-P4VPQ copolymer would have a length of 798.6 nm (C-C bonds, 1.5 Å, 109.28°). When the copolymer formed a bilayer structure, the copolymer molecule was compressed and caused the decreasing of thickness of PB-P4VPQ bilayer[44]. The prediction of the membrane thickness was developed by Helfand and Wasserman et al.[45]

$$t \approx (\gamma a^5 / k_b T)^{1/3} N^b \quad (1)$$

where  $t$  represents the thickness of membrane,  $c$  is the interfacial tension,  $a$  is the length of unit monomers,  $k_b$  is the Boltzmann's constant,  $T$  is temperature,  $N$  designates the number of monomers per copolymer molecule, exponent  $b$  is 0.5 for the copolymer with molecular weight higher than 7 kD. For two different polymers with opposite hydrophilicity, the interfacial tension  $\gamma$  between them has been developed[46]:

$$\gamma = \chi^{1/2} k_b T / a^2 \quad (2)$$

From equations (1) and (2), the thickness of PB-P4VPQ membrane can be calculated to be 12.06 nm[47] ( $T = 293 \text{ K}$ ,  $N = 2218$ ,  $a = 1.5 \text{ Å}$ ).

Figure 8 shows that deposition of 0.1 % PB-P4VPQ solution on silicon oxide substrate would indeed lead to the surface fusion and following vesicles adsorption of the vesicles. The surface histogram analysis of the surface indicates that the difference of the surface roughness between the non-deposited silicon oxide surface and deposited silicon oxide surface was identical. The roughness of the block copolymer membrane was increased after the deposition on the bare silicon oxide surface. The line measurement in Figure 8 (D) shows that the height difference of the copolymer membrane on silicon oxide surface was less than 1 nm, which was much smaller than the thickness of the copolymer bilayer. This measurement indicates that the silicon oxide surface was fully covered by the copolymer membrane. According to figure 8, the vesicles were spread on the surface but the membrane was not “smooth”. We observed several round convex on the surface. This result may be caused by the insufficient density of vesicle deposition even though the property of bilayer membrane is fluid[48] and tends to complement the gap of the non-covered area. The density of deposited vesicles on the unit area of surface might be different, which leads to the different coverage. This analysis also implied that the block copolymer vesicles were spread and fully covered on the silicon oxide surface.

In the bottom-right of Figure 8, we observed a single, non-spread vesicle. The diameter of this vesicle was 140 nm. It may be the vesicle that deposited on the surface after the formation of the block copolymer membrane. Further experiments were performed and will be discussed in the next paragraph.

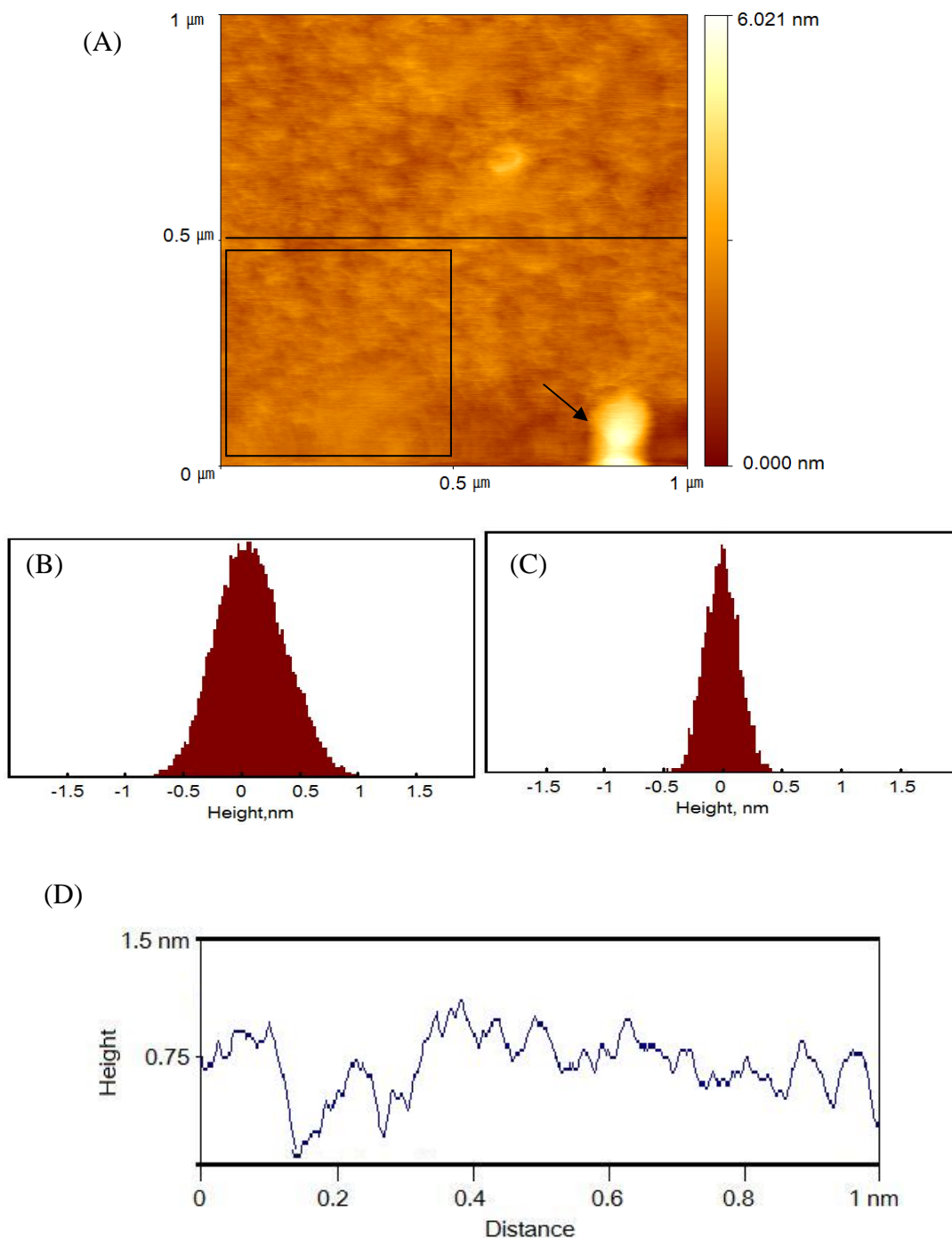
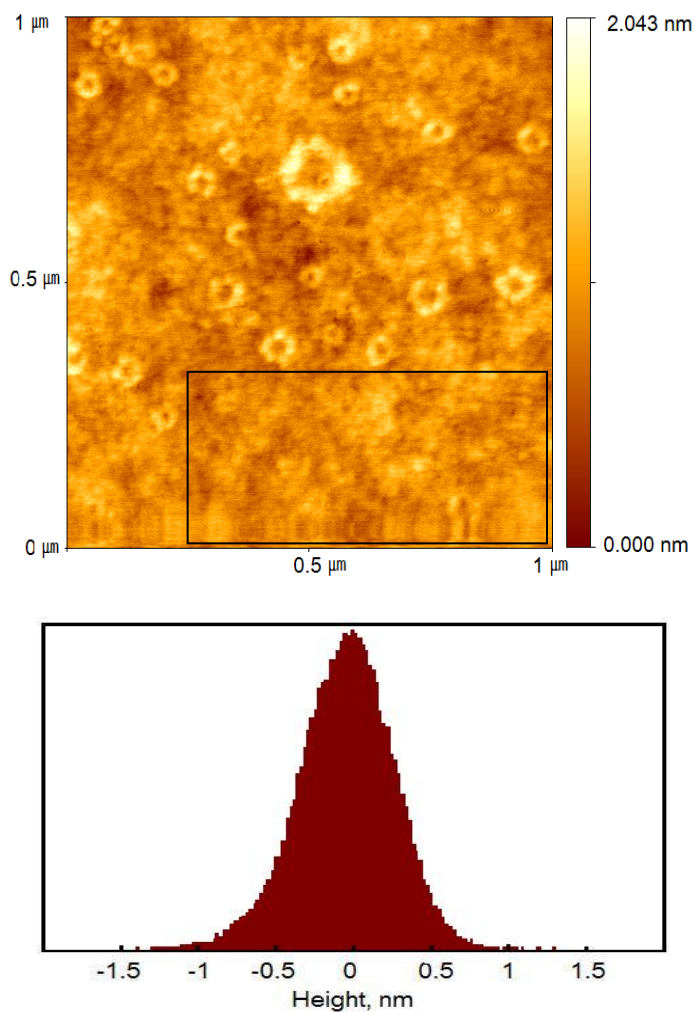


Figure 8. AFM image of the silicon oxide surface deposited the PB-P4VPQ solution. Image (A) deposition of the 0.1 % PB-P4VPQ in THF solution contained 50 % water on the silicon oxide surface. Image revealed a layer of flat vesicular structures. The surface roughness of the background as well as the phase information indicated that the vesicle (bottom right, arrowed) was deposited on the vesicular layer. (B) The surface histogram analysis showed the copolymer layer performed higher surface roughness than bare glass surface (C). (D) The height profile derived from the indicated line.

In order to understand PB-P4VPQ multilayer formation and the morphology of the vesicles deposited on the copolymer membrane, we deposit the vesicle dispersion contained higher concentration of block copolymer on the silicon oxide surface. As shown in Figure 9, the surface histogram analysis suggests a roughness distribution similar to that for the monolayer structure, indicating that the vesicles were spread into a copolymer membrane on the silicon oxide substrate as well. Figure 9 also shows numerous “donut structures” on the surface. Moreover, the histogram analysis of partial surface (Figure 9) was similar to the surface roughness of the previous copolymer membrane (Figure 8). The donut structures indicate that, the PB-P4VPQ vesicles can be spread on the silicon oxide surfaces, but the attractive electrostatic force provided by the block copolymer membrane was not sufficiently strong to disrupt the intra-chain interactions responsible for the integrity of the vesicles. As a result, some vesicles were collapsed and formed donut structures on the copolymer membrane after evaporation of the inner liquid.



*Figure 9. AFM image of the surface deposited the block copolymer vesicular dispersions. Upper image: deposition of the 1 % PB-P4VPQ in THF solution contains 50 % water on the silicon oxide surface. Image revealed numerous collapsed copolymer vesicles (donuts-like structure) on a block copolymer membrane. Lower image: The surface histogram analysis showed the copolymer layer performed higher surface roughness than bare glass surface (Figure 8, (C))*

### 3.3.3 Deposition on muscovite mica

From previous results, we understand that the PB-P4VPQ vesicles would spread on silicon oxide surface in the conditions chosen. However, there are still several

questions that we are interested to address. First, we would like to know what happened during vesicle spreading, what was “partially spread vesicle”. Second, we would like to know the spreading mechanism of block copolymer vesicles on the surface with stronger attractive interaction.

The muscovite mica surface was used since the mica is more hydrophilic than silicon oxide (contact angle  $< 1^\circ$ , table 2) and has the strongest negative charge  $-2 \times 10^{18} \text{ e}^-/\text{m}^2$  [49]. In experiment, 0.1 % of PB-P4VPQ solution was deposited on mica surface for 60 seconds and 120 seconds for the purpose to describe the vesicle spreading mechanism.

Figure 10 shows the deposition of vesicular dispersion on mica surface for 2 minute, the sample was rinsed in order to remove the unattached materials. The surface histogram analysis of the partial surface (Figure 11) shows the difference of the surface roughness between the muscovite mica surface and deposited muscovite mica surface was identical. Therefore, it confirmed the presence of the block copolymer membrane on mica surface. Moreover, the image also showed the presence of several “partial spread vesicles” (arrows). According to the line measurement, the thickness of the overlapped layer was 2.5 – 3.2 nm (Figure 11, (C)). Since the membrane thickness calculated by Helfand and Wasserman equation is 22.16 nm, a film thickness less than 3.2 nm would represent very strong adsorption from the mica surface. The strong attraction resulted in a flat, thinner block copolymer layer. We also observed numerous convex structures on the mica surface. The convex structures have similar height as the partial spread layer, indicating that

these convex structures were also the copolymer bilayer fused from vesicles. Therefore, we concluded that the PB-P4VPQ vesicles tended to fuse and form bilayer membrane on mica surface, and the following vesicles would fuse on the first layer. The “partial spread vesicles” also indicated that the large vesicles (arrows) cannot fully spread on the preexisting copolymer membrane.

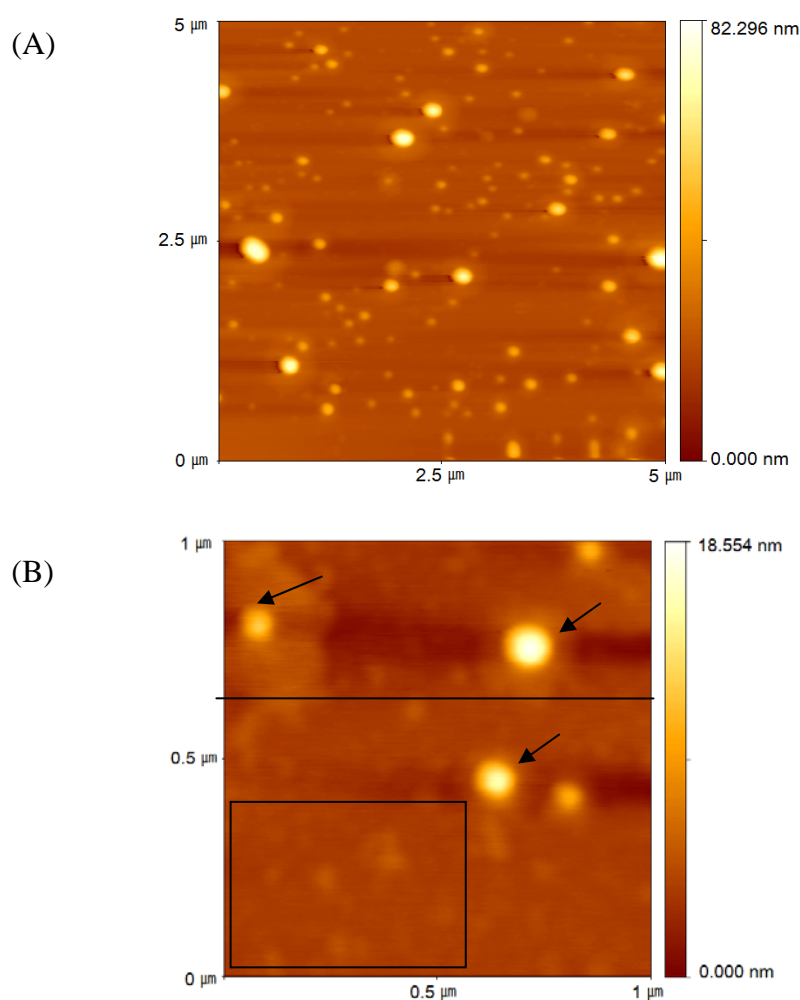


Figure 10. AFM image of the muscovite mica surface after deposited the 0.1 % PB-P4VPQ vesicular dispersion. Solvent: THF solution contains 50 % water. (A) The image of 5  $\mu\text{m}$   $\times$  5  $\mu\text{m}$  dimension. (B) The image of 1  $\mu\text{m}$   $\times$  1  $\mu\text{m}$  dimension. Image revealed numerous “partially spread” vesicular structures on the muscovite mica surface.

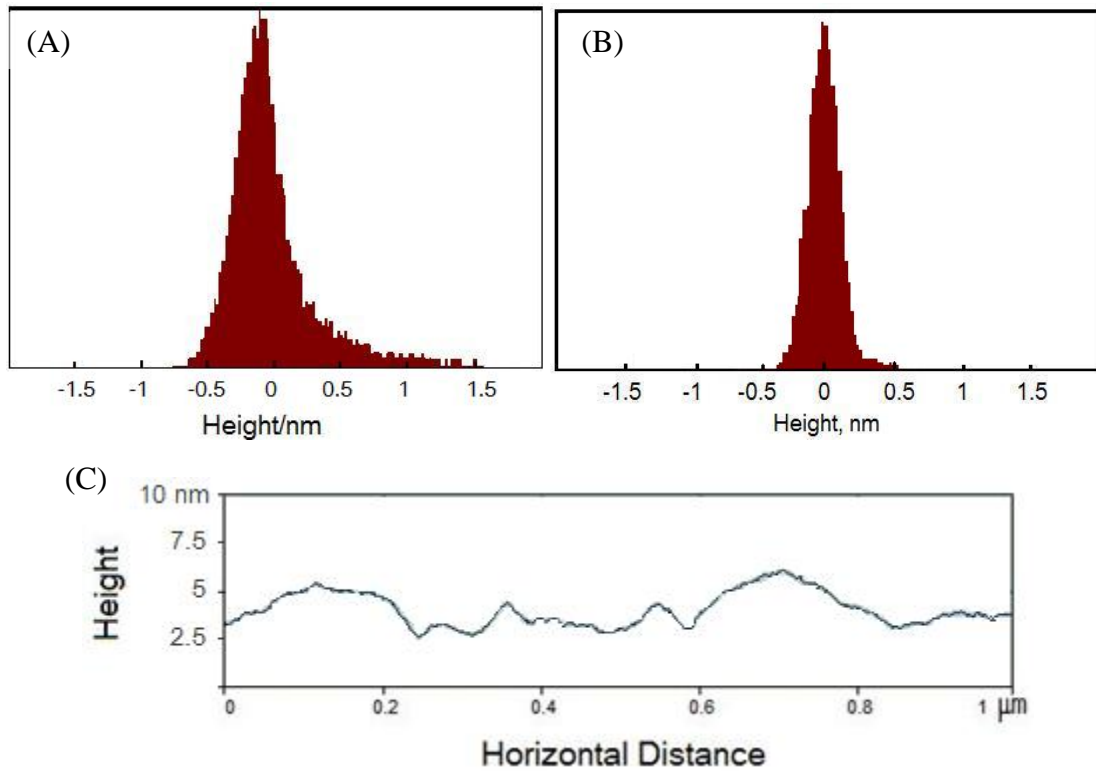


Figure 11. The surface histogram analysis of the mica surface deposited with copolymer vesicular dispersion showed the copolymer layer performed higher surface roughness(A) than bare muscovite mica surface (B). (C) Line measurement of the block copolymer layer on muscovite mica. X-axis indicated the horizontal distance and Y-axis indicates the height difference.

## Conclusions

In this study, we have demonstrated the possibility of fabricating a biomimetic membrane using amphiphilic diblock copolymers by the vesicle fusion method. The morphology of negatively charged copolymer PS-PAA was examined in order to understand the size variance and phase diagram of the self-assembling vesicles. The vesicle size depends on water content and the block copolymer (BCP) concentrations. The spreading of positively charged PB-P4VPQ copolymer vesicles was performed on different surfaces, silicon oxide, muscovite mica and aminoalkylsilane prepared glass. AquaporinZ, a water channel protein, was considered as the candidate for the enzyme reconstitution in biomimetic membrane because of its extraordinary water permeability.

The self-assembly of amphiphilic block copolymer permits a potential of engineering nanoscale superstructures. The critical micelle concentration (CMC) of PS-PAA was between 0.0001 wt% and 0.001 wt% according to our measurements. We observed vesicle phase when the water content exceeded 15 %. The size measurement by dynamic light scattering (DLS) and the morphology on substrate observed by AFM indicated the tendency of size variance; and the size distribution may change section by section. Except the measurements from the systems containing 15 % and 35 % water, the average diameter of vesicles drastically increased when the concentration of BCP reached 1 %.

The fusion behavior of block copolymer vesicles is similar to that of the phospholipid vesicles. We proved the planar PB-P4VPQ membrane can be fabricated by the vesicle fusion method using negative charge substrates such as silicon oxide

and muscovite mica. The membrane formed on silicon oxide surface is near planar, the height difference between the peak and edge of the convex is less than 1.3 nm, indicating the existence of a fully covered block copolymer bilayer. The muscovite mica surface showed strong attraction to the positive charge vesicle. We discovered the overlapping phenomenon of the planar copolymer bilayers and some “partially spread” vesicles on copolymer membranes. In order to engineer a homogeneous film, we found that the silicon oxide surface is suitable for fabricating planar PB-P4VPQ membranes.

The overexpression of AquaporinZ was not succeeded since the membrane proteins tend to maintain a constant amount in live organisms. Besides, the exceeded amount of membrane proteins would decrease the growth rate of cells or even the disruption of the cells. More conditions needed to examine in order to obtain the sufficient amount of Aquaporin.

The block copolymer spreading method can be combined with the membrane protein reconstitution, thus to develop a biomimetic membrane with embedded functional proteins. Toward that end, this study provided some useful preliminary results.

## Reference

1. Bates, F.S. and G.H. Fredrickson, *Block Copolymers---Designer Soft Materials*. Physics Today, 1999. **52** (2) : p. 32-38.
2. Kennedy, J.P., *Developments in block copolymers -1, I. Goodman, ed., applied science (elsevier science) , New York, 1982, 358 pp.* Journal of Polymer Science: Polymer Letters Edition, 1983. **21** (7) : p. 584-585.
3. Luo, L. and A. Eisenberg, *Thermodynamic Size Control of Block Copolymer Vesicles in Solution*. Langmuir, 2001. **17** (22) : p. 6804-6811.
4. Discher, D.E. and A. Eisenberg, *Polymer Vesicles*. Science, 2002. **297** (5583) : p. 967-973.
5. Förster, S. and M. Antonietti, *Amphiphilic Block Copolymers in Structure-Controlled Nanomaterial Hybrids*. Advanced Materials, 1998. **10** (3) : p. 195-217.
6. Vriezema, D.M., et al., *Self-Assembled Nanoreactors*. Chemical Reviews, 2005. **105** (4) : p. 1445-1490.
7. Kataoka, K., A. Harada, and Y. Nagasaki, *Block copolymer micelles for drug delivery: design, characterization and biological significance*. Advanced Drug Delivery Reviews, 2001. **47** (1) : p. 113-131.
8. Hwang, G.-J. and H. Ohya, *Preparation of anion exchange membrane based on block copolymers. Part II: the effect of the formation of macroreticular structure on the membrane properties*. Journal of Membrane Science, 1998. **149** (2) : p. 163-169.
9. Bennett, R.D., et al., *Using Block Copolymer Micellar Thin Films as Templates for the Production of Catalysts for Carbon Nanotube Growth*. Chemistry of Materials, 2004. **16** (26) : p. 5589-5595.
10. Meier, W., C. Nardin, and M. Winterhalter, *Reconstitution of Channel Proteins in (Polymerized) ABA Triblock Copolymer Membranes*. Angewandte Chemie International Edition, 2000. **39** (24) : p. 4599-4602.

11. Kumar, M., et al., *Highly permeable polymeric membranes based on the incorporation of the functional water channel protein Aquaporin Z*. Proceedings of the National Academy of Sciences, 2007. **104** (52) : p. 20719-20724.
12. Chen, Q., H. Schönherr, and G.J. Vancso, *Block-Copolymer Vesicles as Nanoreactors for Enzymatic Reactions*. Small, 2009. **5** (12) : p. 1436-1445.
13. Blanz, A., S.P. Armes, and A.J. Ryan, *Self-Assembled Block Copolymer Aggregates: From Micelles to Vesicles and their Biological Applications*. Macromolecular Rapid Communications, 2009. **30** (4-5) : p. 267-277.
14. Reichert, W.M., C.J. Bruckner, and J. Joseph, *Langmuir-Blodgett films and black lipid membranes in biospecific surface-selective sensors*. Thin Solid Films, 1987. **152** (1-2) : p. 345-376.
15. Chang, J.-F., et al., *Enhanced Mobility of Poly ( $\beta$ -hexylthiophene) Transistors by Spin-Coating from High-Boiling-Point Solvents*. Chemistry of Materials, 2004. **16** (23) : p. 4772-4776.
16. Zhang, S., *Fabrication of novel biomaterials through molecular self-assembly*. Nat Biotech, 2003. **21** (10) : p. 1171-1178.
17. Belegriou, S., et al., *Biomimetic supported membranes from amphiphilic block copolymers*. Soft Matter. **6** (1) : p. 179-186.
18. McConnell, H.M., et al., *Supported planar membranes in studies of cell-cell recognition in the immune system*. Biochimica et Biophysica Acta (BBA) - Reviews on Biomembranes, 1986. **864** (1) : p. 95-106.
19. Watts, T.H., et al., *Antigen presentation by supported planar membranes containing affinity-purified I-Ad*. Proceedings of the National Academy of Sciences of the United States of America, 1984. **81** (23) : p. 7564-7568.
20. Kita-Tokarczyk, K., et al., *Block copolymer vesicles--using concepts from polymer chemistry to mimic biomembranes*. Polymer, 2005. **46** (11) : p. 3540-3563.

21. Gomez-Lagunas, F., et al., *Incorporation of ionic channels from yeast plasma membranes into black lipid membranes*. Biophysical Journal, 1989. **56** (1) : p. 115-119.
22. Tornroth-Horsefield, S., et al., *Structural mechanism of plant aquaporin gating*. Nature, 2006. **439** (7077) : p. 688-694.
23. Dan, N., P. Pincus, and S.A. Safran, *Membrane-induced interactions between inclusions*. Langmuir, 1993. **9** (11) : p. 2768-2771.
24. Cho, I. and Y.-D. Kim, *Formation of stable polymeric vesicles by tocopherol-containing amphiphiles*. Macromolecular Rapid Communications, 1998. **19** (1) : p. 27-30.
25. Pata, V. and N. Dan, *The Effect of Chain Length on Protein Solubilization in Polymer-Based Vesicles (Polymersomes)*. Biophysical Journal, 2003. **85** (4) : p. 2111-2118.
26. Wang, D.-N., et al., *Practical aspects of overexpressing bacterial secondary membrane transporters for structural studies*. Biochimica et Biophysica Acta (BBA) - Biomembranes, 2003. **1610** (1) : p. 23-36.
27. Borgnia, M.J., et al., *Functional reconstitution and characterization of AqpZ, the E. coli water channel protein*. Journal of Molecular Biology, 1999. **291** (5) : p. 1169-1179.
28. Borgnia, M., et al., *CELLULAR AND MOLECULAR BIOLOGY OF THE AQUAPORIN WATER CHANNELS*. Annual Review of Biochemistry, 1999. **68** (1) : p. 425-458.
29. Kaldenhoff, R., et al., *Characterization of Plant Aquaporins*, in *Methods in Enzymology*. 2007, Academic Press. p. 505-531.
30. Soupene, E., et al., *Aquaporin Z of Escherichia coli: Reassessment of Its Regulation and Physiological Role*. J. Bacteriol., 2002. **184** (15) : p. 4304-4307.
31. Tanghe, A., et al., *Aquaporin Expression Correlates with Freeze Tolerance in Baker's Yeast, and Overexpression Improves Freeze Tolerance in Industrial Strains*. Appl. Environ. Microbiol., 2002. **68** (12) : p. 5981-5989.

32. Tang, Z., et al., *Biomedical Applications of Layer-by-Layer Assembly: From Biomimetics to Tissue Engineering*. Advanced Materials, 2006. **18** (24) : p. 3203-3224.
33. Kirby, B.J. and E.F. Hasselbrink, *Zeta potential of microfluidic substrates: 2. Data for polymers*. ELECTROPHORESIS, 2004. **25** (2) : p. 203-213.
34. Bousse, L.J., S. Mostarshed, and D. Hafeman, *Combined measurement of surface potential and zeta potential at insulator/electrolyte interfaces*. Sensors and Actuators B: Chemical, 1992. **10** (1) : p. 67-71.
35. Lian, J., et al., *Improving aquaporin Z expression in Escherichia coli; by fusion partners and subsequent condition optimization*. Applied Microbiology and Biotechnology, 2009. **82** (3) : p. 463-470.
36. Krieger, J., et al., *Expression of an Olfactory Receptor in Escherichia coli: Purification, Reconstitution, and Ligand Binding??AU - Kiefer, Hans*. Biochemistry, 1996. **35** (50) : p. 16077-16084.
37. Ruckenstein, E. and R. Nagarajan, *Critical micelle concentration and the transition point for micellar size distribution*. The Journal of Physical Chemistry, 1981. **85** (20) : p. 3010-3014.
38. Kenneth, D.F. and et al., *The kinetics and mechanism of micelle-vesicle transitions in aqueous solution*. Journal of Physics: Condensed Matter, 1996. **8** (47) : p. 9397.
39. Noguchi, H. and M. Takasu, *Self-assembly of amphiphiles into vesicles: A Brownian dynamics simulation*. Physical Review E, 2001. **64** (4) : p. 041913.
40. Zhang, L. and A. Eisenberg, *Multiple Morphologies of "Crew-Cut" Aggregates of Polystyrene-b-poly (acrylic acid) Block Copolymers*. Science, 1995. **268** (5218) : p. 1728-1731.
41. Shen, H. and A. Eisenberg, *Morphological Phase Diagram for a Ternary System of Block Copolymer PS310-b-PAA52/Dioxane/H2O*. The Journal of Physical Chemistry B, 1999. **103** (44) : p. 9473-9487.

42. Zhao, X., et al., *Solution pH-Regulated Interfacial Adsorption of Diblock Phosphorylcholine Copolymers*. Langmuir, 2005. **21** (21) : p. 9597-9603.
43. Butt, H.J., *Electrostatic interaction in scanning probe microscopy when imaging in electrolyte solutions*. Nanotechnology, 1992. **3** (2) : p. 60.
44. Flory, P.J., *Statistical Thermodynamics of Liquid Mixtures*. Journal of the American Chemical Society, 1965. **87** (9) : p. 1833-1838.
45. Helfand, E. and Z.R. Wasserman, *Block Copolymer Theory. 5. Spherical Domains*. Macromolecules, 1978. **11** (5) : p. 960-966.
46. Battaglia, G. and A.J. Ryan, *Bilayers and Interdigitation in Block Copolymer Vesicles*. Journal of the American Chemical Society, 2005. **127** (24) : p. 8757-8764.
47. Flory, P.J., *Thermodynamics of High Polymer Solutions*. The Journal of Chemical Physics, 1942. **10** (1) : p. 51-61.
48. Haluska, C.K., et al., *Giant Hexagonal Superstructures in Diblock-Copolymer Membranes*. Physical Review Letters, 2002. **89** (23) : p. 238302.
49. Pastr, D., et al., *Adsorption of DNA to Mica Mediated by Divalent Counterions: A Theoretical and Experimental Study*. Biophysical Journal, 2003. **85** (4) : p. 2507-2518.